Hindawi Publishing Corporation
International Journal of Photoenergy
Volume 2012, Article ID 858350, 7 pages
doi:10.1155/2012/858350

Research Article

Current Mechanism in HfO_2-Gated Metal-Oxide-Semiconductor Devices

Osman Pakma

Department of Physics, Faculty of Sciences and Arts, Batman University, 72000 Batman, Turkey

Correspondence should be addressed to Osman Pakma, osman@pakma.com

Received 9 January 2012; Revised 27 March 2012; Accepted 10 April 2012

Academic Editor: Xie Quan

The present study aimed to examine the current density-voltage (J-V) characteristics of Al/HfO_2/p-Si (MOS) structure at temperatures ranging between 100 and 320 K and to determine the structure's current transport mechanism. The HfO_2 film was coated on a single side of the p-Si (111) crystal using the spin coating method. The J-V measurements of the obtained structure at the temperatures between 100 and 320 K revealed that the current transport mechanism in the structure was compatible with the Schottky emission theory. The Schottky emission theory was also used to calculate the structure's Schottky barrier heights (ϕ_B), dielectric constants (ε_r) and refractive index values of the thin films at each temperature value. The dielectric constant and refractive index values were observed to decrease at decreasing temperatures. The capacitance-voltage (C-V) and conductance-voltage (G/ω-V) characteristics of Al/HfO_2/p-Si (MOS) structure was measured in the temperature range of 100–320 K. The values of measured C and G/ω decrease in accumulation and depletion regions with decreasing temperature due to localized N_{ss} at Si/HfO_2 interface.

1. Introduction

As an important group of thin-film electronic materials for microelectronics, dielectrics have a broad range of device applications. They are instrumental both in active devices like transistors and their electrical isolation and in passive devices like capacitors. In these days, when Si-based device technologies are widely put to use, thin film dielectric materials have properties that could be useful in many areas. They have recently been used in both high-permittivity applications such as transistor gate and capacitor dielectrics and low-permittivity materials like inter-level metal dielectrics which operate at switching frequencies in the gigahertz regime for the most demanding applications.

For over forty years, silicon dioxide (SiO_2) films have been preferred for gate dielectric in metal-oxide-semiconductor (MOS) devices. SiO_2 films get thinner in smaller MOS devices. Currently, the technology is aiming to obtain node technologies thinner than 100 nm [1], to which an SiO_2 gate oxide thickness of 1.5–2 nm corresponds. Since direct tunneling has to be made through the thin oxide, high leakage current and reliability problems occur. The solution is high k dielectric materials. A good example for future MOS technologies is HfO_2, while a thickness less than 100 nm in silicon demands a gate dielectric other than SiO_2 [2]. With a high dielectric constant (20–25) and a high band gap (5.1–6.0 eV) [3, 4], it is compatible with polycrystalline silicon gate process and is also thermally stable with silicon [5]. The methods used to prepare HfO_2 thin films have a wide variety. To mention a few, they include Rf magnetron sputtering [6], chemical vapor deposition, and sol-gel process [7, 8]. Of all these methods, the sol-gel method is among the most promising ones because this method could easily control the optical and other properties of thin film when the solution composition and deposition condition are changed.

Thin Hf-layer-coated structures have been reported to include various types of current transport mechanisms, which are Fowler-Nordheim (FN) tunneling, trap-assisted tunneling (TAT), Schottky emission, Poole-Frenkel (PF), direct tunneling (DT), and tunneling-assisted PF emission (TAPF). Pan et al. performed current-voltage (I-V) measurements at high temperatures on HfO_2/TaN-based metal-insulator-metal (MIM) structures whose HfO_2 dielectric material was prepared using the atomic-layer-deposition

(ALD) method, and on the basis of their measurements, they demonstrated that the Schottky emission current dominates in the low-field range of this structure, while the Poole-Frenkel (PF) emission current dominates in its high-field range [9]. As a result of their *I-V* measurements on Al/HfO_2/p-Si metal-oxide-semiconductor structures whose HfO_2 dielectric material was prepared by the RF magnetron sputtering method, Chiu and colleagues reported that the Schottky emission current dominates in the structure at high temperatures and in low-field range, whereas Fowler-Nordheim (FN) tunneling dominates at low temperatures and in high-field range [10].

The present study examined the *I-V* characteristics in a temperature range of 100–320 K of Al/HfO_2/p-Si (MOS) structure whose HfO_2 thin film was prepared by the sol-gel immersion method.

2. Design and Fabrication of Al/HfO_2/p-Si Structures

To prepare the HfO_2 solution, 0.0063 mol hafnium tetrachloride was dissolved in 15 mL ethanol, to which 0.08 mol H_2O and 0.013 mol HNO_3 were added and the solution was kept in a magnetic stirrer for 2 hours. Finally, before coating the film, the solution was kept at 50°C for 4 hours. Several metal-oxide-semiconductor (Al/HfO_2/p-Si) structures were fabricated on the 3-inch diameter float zone <111> p-type (boron-doped) single crystal silicon wafer with a thickness of 600 μm and a resistivity of 5–10 $\Omega\cdot$cm. For the fabrication process, Si wafer was degreased through the RCA cleaning procedure (i.e., a 10-minute boiling in $NH_4OH + H_2O_2 +$ 6 DI (18 MΩ deionised water), which was followed by a 10-minute boiling in HCl + H_2O_2 + 6 DI) [11]. Next, it was subjected to the drying process in N_2 atmosphere for a prolonged time. Following the drying process, high-purity aluminum (99.999%) with a thickness of 1500 Å was thermally evaporated from the tungsten filament onto the whole back surface of the Si wafer under the pressure of 10^{-7} Torr. In order to obtain a low-resistivity ohmic back contact, Si wafer was sintered at 580°C for 3 minutes in N_2 atmosphere. The native oxide on the front surface of the substrate was removed in HF : H_2O (1 : 10) solution, and finally, the wafer was rinsed in deionised water for 30 s before forming an organic layer on the p-type Si substrate. The prepared HFO_2 solution was coated on the shiny side of the cleaned p-Si surface at 2000 rpm by the sol-gel spinning technique. The HfO_2/p-Si structure was annealed for five minutes at 300°C in N_2 atmosphere after each coating process. The procedure was repeated in the same way until the required film thickness was obtained and the structure was finally subjected to annealing at 500°C in N_2 atmosphere for 1 h. The interfacial oxide layer thickness was estimated to be about 8.9 nm by spectroscopic ellipsometry (VASE M2000). In order to obtain a rectifying contact on the front surface of p-Si coated with HfO_2,a high-purity aluminum layer was coated on the surface in a high vacuum under the pressure of 10^{-7} Torr. The Al/HfO_2/p-Si (MOS) structure is given in Figure 1. The current-voltage (*I-V*) characteristics

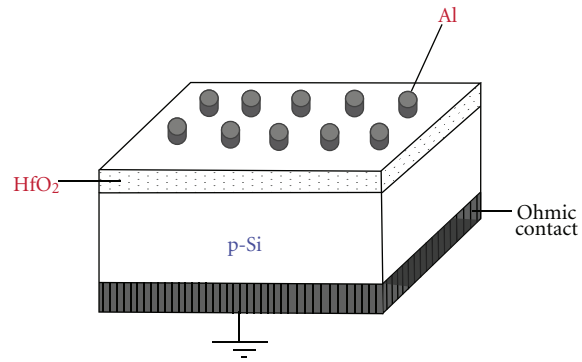

Figure 1: Schematic diagram of Al/HfO_2/p-Si (MOS) structure.

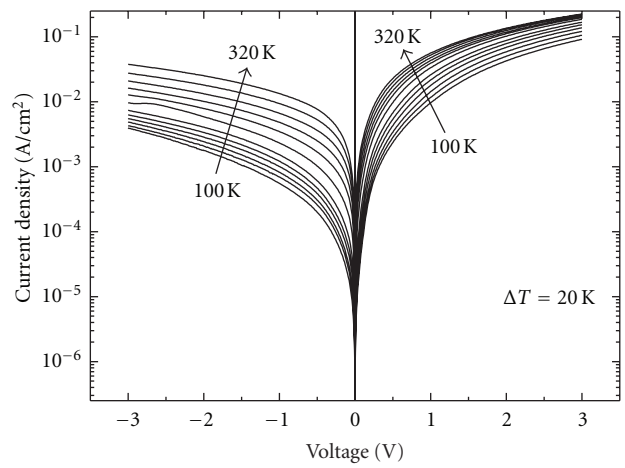

Figure 2: Characteristics of *J-V* plots for Al/HfO_2/p-Si (MOS) structure at various temperatures.

of the samples were measured in the temperature range of 100–320 K using a temperature controlled Janis CCS-350S cryostat, which allowed us to perform the measurements in the temperature range of 10–325 K, and using a Keithley 2420 programmable constant current source under dark conditions. The sample temperature was continually monitored using a GaAlAs sensor and a Lakeshore 330 auto-tuning temperature controller with a sensitivity better than ±0.1 K. The forward and reverse bias capacitance-voltage (*C-V*) and conductance-voltage (*G-V*) measurements were performed in the 1 MHz by using an HP 4192 A LF impedance analyzer (5 Hz to 13 MHz) and the test signal of 50 mV_{rms}. All measurements were carried out in the temperature range of 100–320 K and in the dark.

3. Measurement and Experimental Results

Figure 2 presents the current density-voltage (*J-V*) characteristics of the Al/HfO_2/p-Si (MOS) structure measured in the temperature range of 100–320 K and from −3 V to +3 V. It is found that reverse leakage current density at −1 V is 5.63×10^{-4} A/cm^2 for 100 K and 1.35×10^{-2} A/cm^2 for 320 K, respectively. The reverse bias leakage current was observed to be 26 times higher at 320 K than that of 100 K. It is noted that the leakage current increases with increase

Table 1: The T, n, J_0, and ϕ_B values for the investigated device structure of Figure 3.

T (K)	n	J_0 (A/cm^2)	ϕ_b (eV)
100	4.32	5.50×10^{-06}	0.172
120	3.98	7.36×10^{-06}	0.213
140	3.57	9.35×10^{-06}	0.249
160	3.32	1.40×10^{-05}	0.283
180	2.98	1.96×10^{-05}	0.316
200	2.64	3.04×10^{-05}	0.347
220	2.36	6.64×10^{-05}	0.371
240	2.11	1.28×10^{-05}	0.395
260	1.84	2.67×10^{-05}	0.415
280	1.52	3.49×10^{-05}	0.443
300	1.38	4.62×10^{-05}	0.472
320	1.24	7.12×10^{-05}	0.516

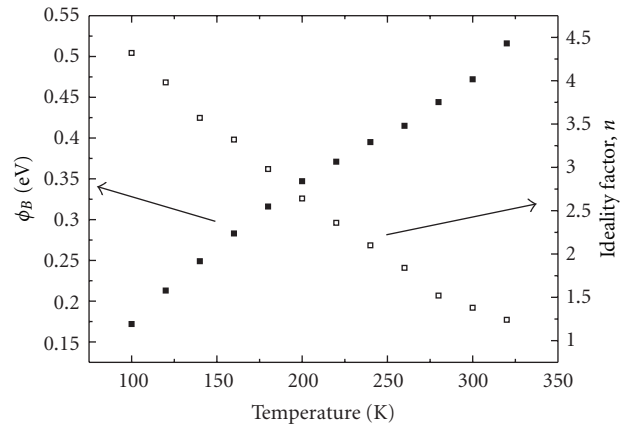

Figure 3: Temperature dependence of the ideality factor and barrier height for the Al/HfO_2/p-Si (MOS) structure.

in temperature. As can be seen in this figure, the ln$J$-V plots are linear on a semilogarithmic scale at low forward bias voltages but deviate considerably from linearity at high forward bias voltages due to the effect of series resistance R_s on the interfacial insulator layer (HfO_2). The current density across an ideal Schottky barrier diode (SBD), based on the thermionic emission (TE) theory, is given by the following relation ($V \geq 3kT/q$) [12]:

$$J = J_0 \exp\left(\frac{q(V - JR_S)}{nkT}\right)\left[1 - \exp\left(-\frac{q(V - JR_S)}{kT}\right)\right], \quad (1)$$

where J_0 is the reverse saturation current density:

$$J_0 = A^* T^2 \exp\left(-\frac{q\phi_B}{kT}\right), \quad (2)$$

where ϕ_B, R_S, A^*, n, q, and T are the zero bias barrier height, series resistance of structure, the effective Richardson constant (32 A/cm^2 K^2 for p-type Si [12]), the ideality factor, the electron charge, and the temperature in Kelvin, respectively.

As it is known, the characteristic ln$J$-V graph of a diode usually has three regions, which are low-voltage region ($V \leq 0.1$ V), medium-voltage region (0.1 V $\leq V \leq 0.8$ V), and high-voltage region ($V \geq 0.8$ V), respectively. The electrical parameters except for R_s were calculated in the linear region in the medium voltage region, while R_s was calculated in the region where the ln$J$-V curve in the high-voltage region bended. As can be seen from Figure 2, each semilogarithmic J-V curve consists of a linear range with different slopes in between the intermediate-bias voltage (0.07 V $\leq V \leq 0.7$ V) regions. The experimental values of n and ϕ_B were determined from (1) and (2), respectively, and they are shown at each temperature in Table 1. As can be seen in Table 1, the values of n and ϕ_B range from 1.24 and 0.516 eV (320 K) to 4.32 and 0.172 eV (100 K), respectively. Both parameters exhibit a strong temperature dependency as seen in Figure 3. As seen from Figure 3, while n increased, ϕ_B decreased with decreasing temperature.

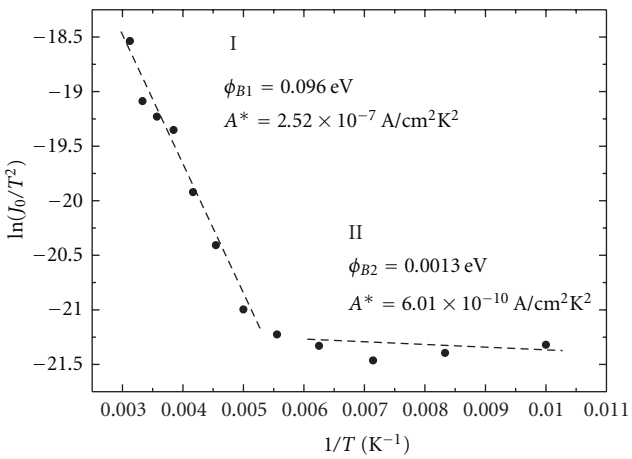

Figure 4: Richardson plots of the ln(J_0/T^2) versus 1/T for the Al/HfO_2/p-Si (MOS) structure.

Because of the temperature-activated process, the current transport will be dominated by current flowing through the lower BH and a larger ideality factor [13]. That is, more electrons have sufficient energy to overcome the higher barrier when temperature increases, and then, BH increases with temperature and bias voltage.

Figure 4 shows the conventional Richardson (ln(J_0/T^2) versus 1/T plot. The Richardson constant and effective barrier height at 0 K are obtained from the intercept and slope of linear fit. ln(J_0/T^2) versus 1/T plot has two linear temperature ranges. In the first region (180–320 K), the values of effective barrier height obtained from the slope of this straight line come out to be 0.096 eV. Likewise, the value Richardson constant determined from the intercept at the ordinate is 2.52×10^{-7} A/cm^2 K^2. In the second region (100–160 K), the values of effective barrier height and Richardson constant were derived from the slope and intercept of this straight line as 0.0013 eV and 6.01×10^{-10} A/cm^2 K^2, respectively. The Richardson constant values are much lower than the known value of 32 A/cm^2 K^2 for p-type Si. As explained before, the deviation in the Richardson plots might

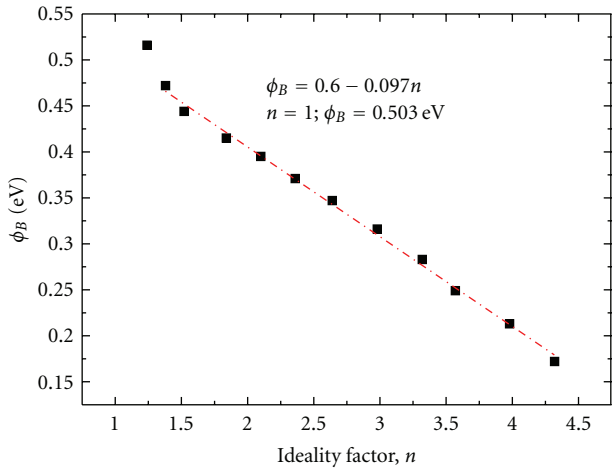

Figure 5: Barrier height versus ideality factor of the Al/HfO_2/p-Si (MOS) structure at various temperatures.

be a result of the spatially inhomogeneous barrier heights and potential fluctuations at the interface, which consist of low and high barrier areas [14–17].

Figure 5 shows a plot of the experimental barrier height versus the ideality factor for various temperatures. As can be seen in Figure 5, there are linear regions between the experimental barrier heights and ideality factors of the Al/HfO_2/p-Si (MOS) structure, which can be explained by lateral inhomogeneities of the barrier heights [14, 17]. The exploration of the experimental barrier height versus the ideality factor plot to $n = 1$ has given a value of 0.503 eV, which is close to half of the band gap in Si. These results confirm that the predominant current transport is not the TE in our samples.

The standard Schottky emission equation is as follows [12]:

$$J = A^* T^2 \exp\left[\frac{-q\left(\phi_B - \sqrt{qE/4\pi\varepsilon_r\varepsilon_0}\right)}{kT}\right], \qquad (3)$$

where $A^* = 4\pi q(m^*_{ox})k^2/h^3 = 120(m^*_{ox}/m_0)$ (A/cm^{2}K^2), A^* is the effective Richardson constant, q is the electronic charge, E is the electric field, h is Planck's constant, ε_0 is the permittivity of free space, ε_r is the dynamic dielectric constant, m_0 is the free electron mass, and m^*_{ox} is the electron effective mass in HfO_2 ($m^*_{ox} = 0.4$ for Al/HfO_2 and $m^*_{ox} = 0.18$ for HfO_2/Si) [5, 18].

For the standard Schottky emission, a plot of $\ln(J/T^2)$ versus $E^{1/2}$ should be linear. As seen in Figures 6 and 7, there is a very good fit between the experimental data in the region for each measurement temperature and high electric field and the Schottky emission theory for both gate injection and substrate injection. At each temperature in Table 2, the experimental refractive index values ($n = \varepsilon_r^{1/2}$), ε_r and ϕ_B were determined from (3), respectively. Table 2 reveals that experimentally determined dynamic dielectric constants at room temperature in standard Schottky plots are so close to 4, the square of the refractive index 2 [3, 19]. This points out to the consistency between the conduction mechanism

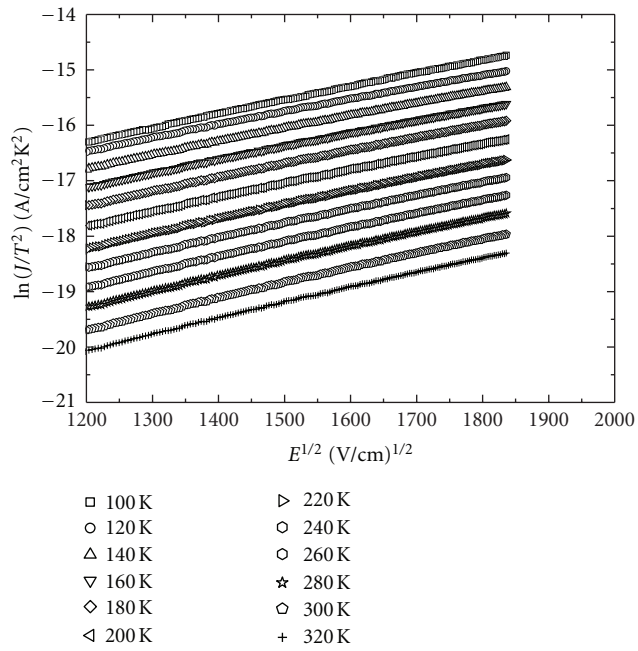

Figure 6: Characteristics of Schottky emission in the region of high field under gate injection.

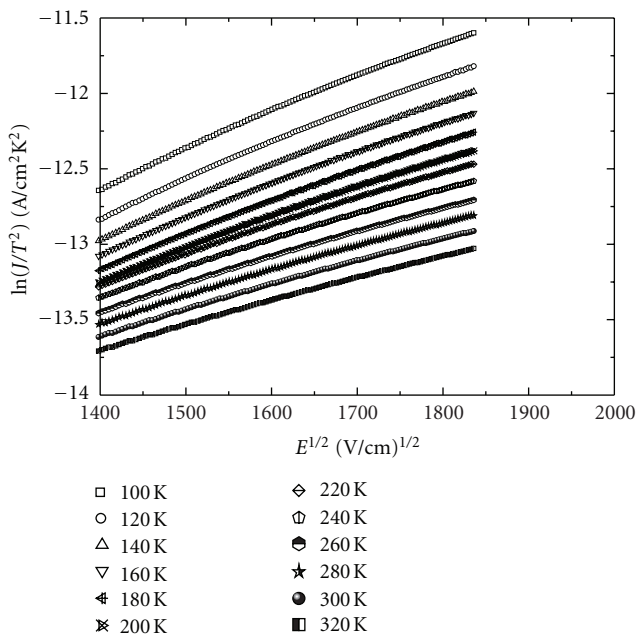

Figure 7: Characteristics of Schottky emission in the region of high field under substrate injection.

under high electric fields and Schottky emission. Another observation was that the extracted refractive index value gradually increases with increased measurement temperature, which may result from the effects of thermal stress, thermal expansion, and electronic polarizability [20–22]. The barrier height at the Al/HfO_2 and HfO_2/p-Si interfaces was determined from 0.482 and 0.342 eV (100 K) to 0.936 and 0.778 eV (320 K), respectively.

Table 2: Temperature-dependent values of various parameters obtained from the J-V characteristics of the Al/HfO_2/p-Si structure.

T (K)	Gate injection			Substrate injection		
	ϕ_b (eV)	n	ε_r	ϕ_b (eV)	n	ε_r
100	0.482	1.71	2.92	0.342	1.66	2.75
120	0.522	1.72	2.96	0.387	1.67	2.79
140	0.561	1.72	2.97	0.431	1.68	2.83
160	0.602	1.73	3.01	0.474	1.70	2.88
180	0.641	1.76	3.09	0.516	1.71	2.92
200	0.683	1.77	3.13	0.556	1.72	2.97
220	0.725	1.79	3.19	0.591	1.74	3.03
240	0.763	1.80	3.24	0.627	1.76	3.10
260	0.807	1.81	3.27	0.666	1.77	3.15
280	0.850	1.82	3.32	0.703	1.79	3.22
300	0.895	1.84	3.38	0.739	1.81	3.29
320	0.936	1.85	3.41	0.778	1.83	3.36

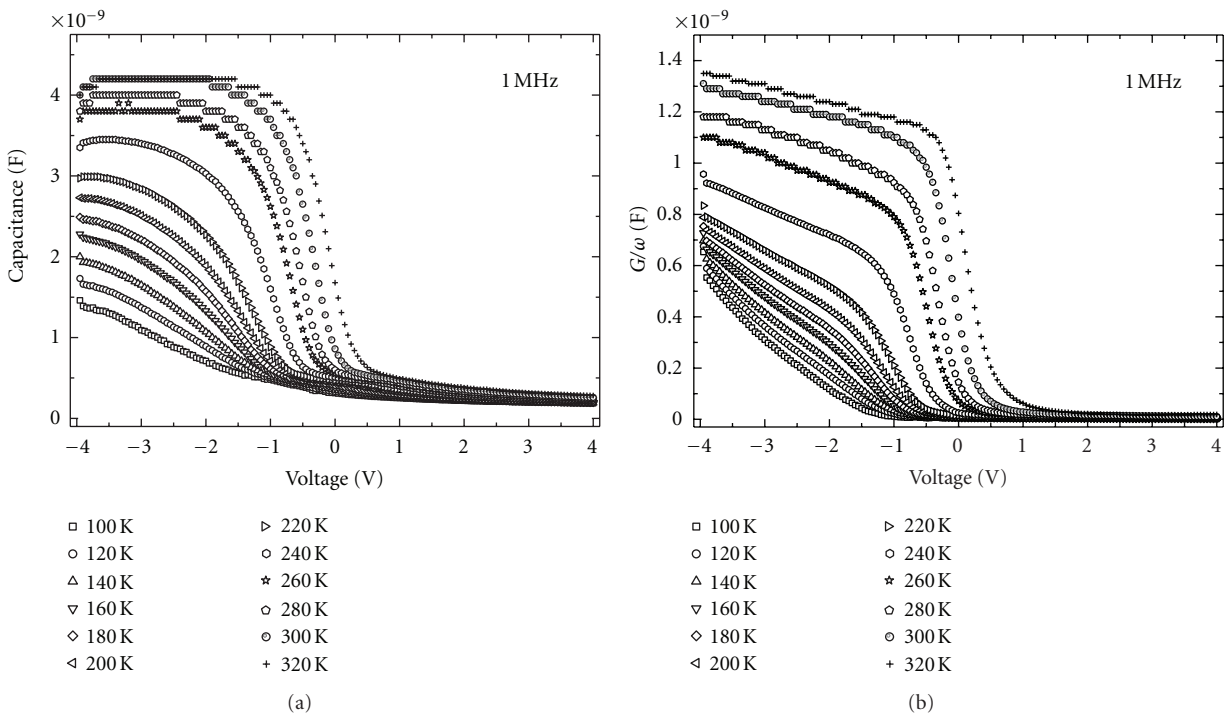

Figure 8: The temperature-dependent curves of the (a) C-V and (b) G/ω-V characteristics of Al/HfO_2/p-Si (MOS) structure as measured at 1 MHz.

There are a number of suggested methods which help to extract the R_s of structure, and among them the most important one is the conductance method, developed by Nicollian and Goetzberger [23–26]. In this method, the frequency-dependent forward and reverse bias C-V and G/ω-V measurements give the detail information on the distribution profile of R_s of MOS structure. When the MOS structure is biased into strong accumulation, the impedance ($Z_{ma} = 1/Y_{ma}$) is given by [23]

$$Z_{ma} = \frac{1}{G_{ma} + j\omega C_{ma}}, \tag{4}$$

where C_{ma} and G_{ma} are the measured capacitance and conductance, in strong accumulation region. Series resistance is the real part of the impedance ($Z_{ma} = 1/Y_{ma}$) or

$$R_S = \frac{G_{ma}}{G_{ma}^2 + (\omega C_{ma})^2}. \tag{5}$$

The oxide layer capacitance (C_{ox}) is obtained by substituting R_s from (5) into the following relations:

$$C_{ox} = C_{ma}\left[1 + \left(\frac{G_{ma}}{\omega C_{ma}}\right)^2\right] = \frac{\varepsilon_i \varepsilon_0 A}{\delta}, \tag{6}$$

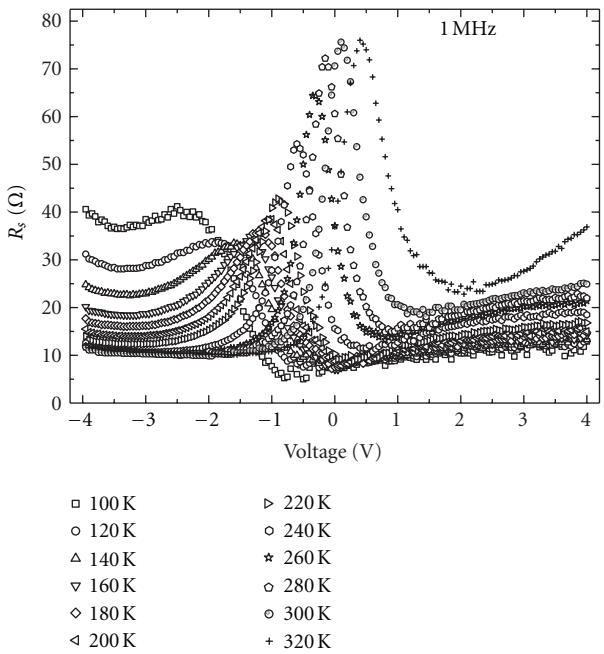

Figure 9: The variation of the series resistance of the Al/HfO_2/p-Si (MOS) structure as a function of the bias voltage for various temperatures.

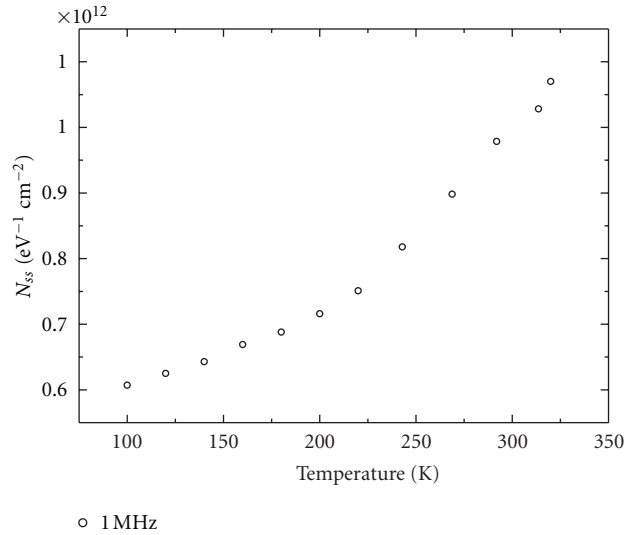

Figure 10: The interface states of the Al/HfO_2/p-Si (MOS) structure as measured at 1 MHz for various temperatures.

where C_m and G_m are the capacitance and conductance measured across the MOS structure at any bias voltage.

The capacitance-voltage (C-V) and conductance-voltage (G/ω-V) characteristics of Al/HfO_2/p-Si (MOS) structure were measured in the temperature range of 100–320 K (1 MHz) and are given in Figures 8(a) and 8(b), respectively. As can be seen from Figures 8(a) and 8(b) both curves have three distinct regimes of accumulation-depletion-inversion. The values of measured C and G/ω decrease in accumulation and depletion regions with decreasing temperature due to localized N_{ss} at Si/HfO_2 interface. Such behavior of the C and G/ω is attributed to particular distribution of interface states at p-Si/HfO_2 interfaces and R_s of structure [23].

Using (5) the values of R_s were calculated as a function of bias in the temperature range of 100–320 K and are given in Figure 9. As can be clearly seen from Figure 9, the R_s gives a peak. The peak position of R_s is shifting toward inversion region with increasing temperature. Such behavior of R_s is attributed to the particular distribution of localized N_{ss} at p-Si/HfO_2 interface states and interfacial insulator layer at Al/p-Si interface.

The density of interface states (N_{ss}) at p-Si/HfO_2 can be derived from Hill-Coleman method [27]. According to this method, N_{ss} is given by

$$N_{SS} = \frac{2}{qA} \frac{(G_m/\omega)_{\max}}{((G_m/\omega)_{\max}/C_{\text{ox}})^2 + (1 - (C_m/C_{\text{ox}}))^2}, \qquad (7)$$

where A is the area of the structure, and $(G_m/\omega)_{\max}$ is the maximum measured conductance value. Figure 10 shows that the N_{ss} increase with increasing temperature. The high values of C and G at high temperatures were attributed to the excess capacitance resulting from the N_{ss}, which is in equilibrium with the semiconductor that follows the ac signal.

4. Conclusions

The forward and reverse J-V, C-V, and G/ω-V characteristics of Al/HfO_2/p-Si (MOS) structure derived using the sol-gel method were measured at temperatures ranging between 100 and 320 K. The J-V measurements of the obtained Al/HfO_2/p-Si (MOS) structure at the temperatures between 100 and 320 K revealed that the current transport mechanism in the structure was compatible with the Schottky emission theory. The Schottky emission theory was also used to calculate the structure's Schottky barrier heights (ϕ_B), dielectric constants (ε_r), and refractive index values of the thin films at each temperature value. The dielectric constant and refractive index values were observed to decrease at decreasing temperatures. The values of measured C and G/ω decrease in accumulation and depletion regions with decreasing temperature due to localized N_{ss} at Si/HfO_2 interface. The N_{ss} increase with increasing temperature.

References

[1] R. K. Nahar, V. Singh, and A. Sharma, "Study of electrical and microstructure properties of high dielectric hafnium oxide thin film for MOS devices," *Journal of Materials Science*, vol. 18, no. 6, pp. 615–619, 2007.

[2] *International Technology Road Map for Semiconductors*, San-Jose, Calif, USA, 1999.

[3] M. Balog, M. Schieber, M. Michman, and S. Patai, "Chemical vapor deposition and characterization of HfO_2 films from organo-hafnium compounds," *Thin Solid Films*, vol. 41, no. 3, pp. 247–259, 1977.

[4] M. Housa, *High k Gate Dielectric*, IPO, Bristal, 2004.

[5] F. C. Chiu, "Interface characterization and carrier transportation in metal/ HfO_2/silicon structure," *Journal of Applied Physics*, vol. 100, no. 11, Article ID 114102, 2006.

[6] L. Khomenkova, X. Portier, J. Cardin, and F. Gourbilleau, "Thermal stability of high-k Si-rich HfO_2 layers grown by RF magnetron sputtering," *Nanotechnology*, vol. 21, no. 28, Article ID 285707, 2010.

[7] Y. Ohshita, A. Ogura, A. Hoshino, S. Hiiro, T. Suzuki, and H. Machida, "Using tetrakis-diethylamido-hafnium for HfO_2 thin-film growth in low-pressure chemical vapor deposition," *Thin Solid Films*, vol. 406, no. 1-2, pp. 215–218, 2002.

[8] Y. Aoki, T. Kunitake, and A. Nakao, "Sol-gel fabrication of dielectric HfO_2 nano-films; formation of uniform, void-free layers and their superior electrical properties," *Chemistry of Materials*, vol. 17, no. 2, pp. 450–458, 2005.

[9] S. Pan, S. J. Ding, Y. Huang et al., "High-temperature conduction behaviors of HfO_2/TaN-based metal-insulator-metal capacitors," *Journal of Applied Physics*, vol. 102, no. 7, Article ID 073706, 2007.

[10] F. C. Chiu, S. A. Lin, and J. Y. M. Lee, "Electrical properties of metal-HfO_2-silicon system measured from metal-insulator-semiconductor capacitors and metal-insulator-semiconductor field-effect transistors using HfO_2 gate dielectric," *Microelectronics Reliability*, vol. 45, no. 5-6, pp. 961–964, 2005.

[11] W. Kern, *Handbook of Semiconductor Cleaning Technology*, Noyes, New York, NY, USA, 1993.

[12] S. M. Sze and K. Ng Kwok, *Physics of Semiconductor Devices*, Wiley, Hoboken, NJ, USA, 3nd edition, 2007.

[13] R. F. Schmitsdorf, T. U. Kampen, and W. Mönch, "Explanation of the linear correlation between barrier heights and ideality factors of real metal-semiconductor contacts by laterally nonuniform Schottky barriers," *Journal of Vacuum Science and Technology B*, vol. 15, no. 4, pp. 1221–1226, 1997.

[14] Ş. Karataş, Ş. Altindal, A. Türüt, and A. Özmen, "Temperature dependence of characteristic parameters of the H-terminated Sn/p-Si(1 0 0) Schottky contacts," *Applied Surface Science*, vol. 217, no. 1–4, pp. 250–260, 2003.

[15] E. Dobročka and J. Osvald, "Influence of barrier height distribution on the parameters of Schottky diodes," *Applied Physics Letters*, vol. 65, no. 5, pp. 575–577, 1994.

[16] F. E. Jones, B. P. Wood, J. A. Myers, C. Daniels-Hafer, and M. C. Lonergan, "Current transport and the role of barrier inhomogeneities at the high barrier *n*-InP | poly(pyrrole) interface," *Journal of Applied Physics*, vol. 86, no. 11, pp. 6431–6441, 1999.

[17] M. C. Lonergan and F. E. Jones, "Calculation of transmission coefficients at nonideal semiconductor interfaces characterized by a spatial distribution of barrier heights," *Journal of Chemical Physics*, vol. 115, no. 1, pp. 433–445, 2001.

[18] Y. T. Hou, M. F. Li, H. Y. Yu, and D. L. Kwong, "Modeling of tunneling currents through HfO_2 and $(HfO_2)_x(Al_2O_3)_{1-x}$ gate stacks," *IEEE Electron Device Letters*, vol. 24, no. 2, pp. 96–98, 2003.

[19] H. W. Chen, F. C. Chiu, C. H. Liu et al., "Interface characterization and current conduction in HfO_2-gated MOS capacitors," *Applied Surface Science*, vol. 254, no. 19, pp. 6112–6115, 2008.

[20] W. H. Cheng, S. F. Chi, and A. K. Chu, "Effect of thermal stresses on temperature dependence of refractive index for Ta_2O_5 dielectric films," *Thin Solid Films*, vol. 347, no. 1-2, pp. 233–237, 1999.

[21] C. Z. Tan, "Review and analysis of refractive index temperature dependence in amorphous SiO_2," *Journal of Non-Crystalline Solids*, vol. 238, no. 1-2, pp. 30–36, 1998.

[22] S. J. Ding, J. Xu, Y. Huang, Q. Q. Sun, D. W. Zhang, and M. F. Li, "Electrical characteristics and conduction mechanisms of metal-insulator-metal capacitors with nanolaminated Al_2O_3-HfO_2 dielectrics," *Applied Physics Letters*, vol. 93, no. 9, Article ID 092909, 2008.

[23] E. H. Nicollian and J. R. Brews, *Metal-Oxide Semiconductor (MOS) Physics and Technology*, Wiley, New York, NY, USA, 1982.

[24] H. Norde, "A modified forward I-V plot for Schottky diodes with high series resistance," *Journal of Applied Physics*, vol. 50, no. 7, pp. 5052–5053, 1979.

[25] K. Sato and Y. Yasumura, "Study of forward I-V plot for Schottky diodes with high series resistance," *Journal of Applied Physics*, vol. 58, no. 9, pp. 3655–3657, 1985.

[26] S. K. Cheung and N. W. Cheung, "Extraction of Schottky diode parameters from forward current-voltage characteristics," *Applied Physics Letters*, vol. 49, no. 2, pp. 85–87, 1986.

[27] W. A. Hill and C. C. Coleman, "A single-frequency approximation for interface-state density determination," *Solid-State Electronics*, vol. 23, no. 9, pp. 987–993, 1980.